Rare Metal Materials and Engineering
Volume 50, Issue 10, October 2021
Available online at www.rmme.ac.cn

Science Press

Cite this article as: Yuan Shuai, Jia Lina, Zhang Hu. Effects of Er on the Microstructure and Eutectic Phase Morphology of Directionally Solidified Al-Zn-Mg-Cu-Zr Alloys[J]. Rare Metal Materials and Engineering, 2021, 50(10): 3477-3484.

ARTICLE

Effects of Er on the Microstructure and Eutectic Phase Morphology of Directionally Solidified Al-Zn-Mg-Cu-Zr Alloys

Yuan Shuai, Jia Lina, Zhang Hu

School of Materials Science and Engineering, Beihang University, Beijing 100191, China

Abstract: Four alloy rods of Al-Zn-Mg-Cu-Zr-*x*Er (*x*=0, 0.1, 0.2, 0.5, wt%) were prepared by directional solidification. The microstructure and second phase morphology of alloys were investigated by optical microscopy (OM), electron probe micro-analysis (EPMA), energy dispersive spectrometer (EDS) and other methods. The results indicate that Er element can increase the number of dendrites in the directional solidification structure of Al-Zn-Mg-Cu-Zr alloy, and reduce the primary dendrite arm spacing and secondary dendrite arm spacing of the alloy. A proper amount of Er element can reduce the content of second phase in the alloy and increase the tendency to form round second phase. The formation of Al_8Cu_4Er phase can reduce the Cu content in the T phase (AlZnMgCu phase), which plays a role of rounding the boundary of the T phase, and can change the morphology and internal structure of the T phase. The Al_8Cu_4Er phase serves as the nucleation position of the T phase, and part of the T phase grows around this phase. The addition of Er can improve the microhardness of the alloy.

Key words: Al-Zn-Mg-Cu; Er; microstructure; eutectic phase; second phase morphology

Ultra-high-strength Al-Zn-Mg-Cu series alloy (7xxx series aluminum alloy) has become a very popular aluminum alloy series due to its advantages of high strength, high hardness, light mass, easy processing and excellent thermal conductivity. It is widely used in aerospace industry and military fields. Therefore, Al-Zn-Mg-Cu series aluminum alloy occupies an important position in the fields of national defense, military, and people's daily life[1-8].

In order to improve the comprehensive performance of the Al-Zn-Mg-Cu series alloy, many material workers have added different trace elements to the 7xxx series aluminum alloy. Among them, Er element has gradually entered the material workers' vision due to its relatively cheap price and good micro-alloying effect. Wang et al[9] studied the effect of Er on the structure of Al-Zn-Mg-Cu alloy in as-cast and homogenized states, and found that after adding 0.5wt% Er, the grain size of the alloy increases and the grains become coarse dendrites. During the solidification of the alloy, most of the Er formed the ternary alloy phase Al_8Cu_4Er at the grain boundary. Since the remelting temperature of the Al_8Cu_4Er phase is about 575 ℃, the homogenization treatment cannot effectively eliminate the Al_8Cu_4Er phase. Wu et al[10] observed the effect of homogenization heat treatment on the precipitation of $Al_3(Er,Zr)$ particles and grain recrystallization behavior in Al-Zn-Mg-Zr-Er alloy, and the results showed that compared with the traditional single-stage homogenization, two-stage homogenization and ramp heating homogenization can obtain finer $Al_3(Er, Zr)$ particles, higher particle number density and volume fraction. Wu et al [11] investigated the microstructure evolution of the Er, Zr microalloyed Al-Zn-Mg-Cu alloy during homogenization heat treatment, and obtained a relatively reasonable alloy homogenization heat treatment system. In addition, a trace amount of Er can refine the alloy grains, improve the mechanical properties of the alloy, and significantly improve the alloy's resistance to intergranular corrosion and stress corrosion in Al-Zn-Mg-Cu alloys[12,13].

For Al-Zn-Mg-Cu series alloys, the use of products should go through the processes of ingot casting, homogenization heat treatment, heat deformation processing, solid solution and aging heat treatment. In different process stages, the microstructure of alloy and morphology of the second phase are different, which may have different effects on the next

Received date: October 10, 2020
Foundation item: National Key Research and Development Program of China (2016YFB0300901)
Corresponding author: Jia Lina, Ph. D., School of Materials Science and Engineering, Beihang University, Beijing 100191, P. R. China, Tel: 0086-10-82316958, E-mail: jialina@buaa.edu.cn

process and the performance of the final product. Mehdi Malekan et al[14] found that although both Ni and Cr can improve the mechanical properties of the alloy, the alloying effect of Ni is better than that of Cr. This is because Al_3Ni precipitated in the alloy is in the form of fine fragments, while Al_7Cr is irregular polygon, and the boundary is relatively sharp, which affect the performance of the alloy. The microstructure of the initial ingot of Al-Zn-Mg-Cu series alloy and the composition, morphology and quantity of the second phase are the basis of the whole process flow, which often play a decisive role in the final properties of the material. At present, the research of Al-Zn-Mg-Cu series alloy mainly focuses on the effects of homogenization heat treatment, hot deformation processing, solution quenching, aging heat treatment on the microstructure evolution and comprehensive properties of the alloy. Nevertheless, there are few studies on the as-cast structure of the alloy. Therefore, it is necessary to analyze the second phase morphology in the as-cast structure[15-25].

The second phases precipitated in Al-Zn-Mg-Cu alloys are generally the products of eutectic reaction, such as T phase (AlZnMgCu phase), θ phase (Al_2Cu phase)[26-29]. In addition, the eutectic reaction can be better carried out under the condition of directional solidification[30], which can more intuitively reflect the influence of alloy elements on the primary dendrite arm spacing and secondary dendrite arm spacing. Therefore, in this study, a directional solidification method was used to analyze the solidification structure of alloys with four different compositions of Al-Zn-Mg-Cu-Zr-*x*Er (*x*=0, 0.1, 0.2, 0.5, wt%). The influence of alloy chemical composition difference on its solidified micro-structure and the formation process of different solidified precipitates was discussed. The influence of different content of Er element on the precipitated phase type, morphology and distribution of the alloy solidified structure was revealed. The alloying mechanism and action of Er in the solidification process of Al-Zn-Mg-Cu aluminum alloy were also determined.

1 Experiment

Four Al-Zn-Mg-Cu-Zr alloys containing Er elements with different mass fractions were used in the experiment. The nominal chemical compositions of alloys were Al-9.0Zn-2.1Mg-2.1Cu-0.13Zr-*x*Er (*x*=0, 0.1, 0.2, 0.5, wt%), named as alloy 1, alloy 2, alloy 3, and alloy 4, respectively. The raw materials were aluminum blocks, zinc sections, magnesium blocks with a purity of 99.99%, Al-50Cu intermediate alloys, Al-10Zr intermediate alloys and Al-20Er intermediate alloys, which were repeatedly smelted in a vacuum arc furnace for 4 times and then cast into a master alloy ingot with a mass of about 700 g. Each alloy was cut by wire cutting to obtain two sample rods with a diameter of 12 mm and a length of 100 mm. After removing the surface oxide scale, they were ultrasonically cleaned with acetone, then dried, and filled into an Al_2O_3 ceramic tube with an inner diameter of 12 mm and a length of 210 mm. The Bridgman type liquid metal cooling directional solidification furnace was evacuated to 6.0×10^{-3} Pa, then filled with high-purity Ar to 0.5×10^5 Pa. A tungsten cylinder resistance was used to heat the temperature to 750 °C (W-Re thermocouple temperature measurement at about 100 mm above the furnace heat insulation plate), and the directional solidification experiment was carried out after 60 min of heat preservation. The drawing rate was selected to be 100 μm/s.

The directional solidification rod was split in the middle along the drawing direction, one half was used to observe the cross-sectional structure, and the other half was used to observe the longitudinal cross-sectional structure of different solidification positions. Carl Zeiss metallographic microscope, JXA-8100 type electron probe micro-analysis (EPMA) and attached INCA energy spectrometer (EDS) were used to investigate the microstructure and phase composition of the alloys, and the hardness of the alloys was measured by FM800 micro-Vickers hardness tester. Image Pro Plus 6.0 professional image analysis software was was to count the size and area fraction of microstructure. The corrosive agent was Keller reagent (95 mL H_2O+2.5 mL HNO_3+1.5 mL HCl+1.0 mL HF) and Weck reagent (100 mL H_2O+5 g $KMnO_4$+1 g NaOH).

2 Results

2.1 Microstructure evolution in Al-Zn-Mg-Cu-Zr-(Er) alloys

Fig. 1 shows the microstructure of Al-Zn-Mg-Cu-Zr alloys with different Er contents. It can be seen that the alloys added with different contents of Er element are all dendritic structures, which are mainly composed of primary dendrites and less developed secondary dendrite arms. A large number of continuous dendrites are formed in alloy 4, which might have a negative impact on the mechanical properties. The color metallography was used to measure the primary and secondary dendrite arm spacing. The specific measurement method is shown in Fig. 1i. The distances were measured 30 times and the average value was taken. The primary and secondary dendrite arm spacing of four alloys were statistically analyzed. The results are displayed in Fig. 2. The grains of alloy 1 are the coarsest, whose primary and secondary dendrite arm spacings are much larger than those of other Er-containing alloys. As the Er content increases, the grain size of the alloys becomes smaller, and the primary dendrite arm spacing and the secondary dendrite arm spacing decrease accordingly. The primary dendrite arm spacing decreases from 237.3 μm of alloy 1 to 146.5 μm of alloy 4. The distance between the secondary dendrite arms is reduced from 61.8 μm in alloy 1 to 44.6 μm in alloy 4.

Fig. 3 shows the backscattered electron images of alloys with different Er contents. The second phase precipitated in the alloy was analyzed by EDS. The results are shown in Table 1. Among them, the precipitated phases in alloy 1 are mainly T phase (AlZnMgCu), the precipitated phases in alloy 2, alloy 3, and alloy 4 added with Er are mainly Al_8Cu_4Er phase and T phase, and the two phases are connected. Otherwise, a certain amount of Zn is found in the Al_8Cu_4Er phase, which will be discussed later.

2.2 Second phase analysis

Fig. 3 shows that as the Er content increases, the number

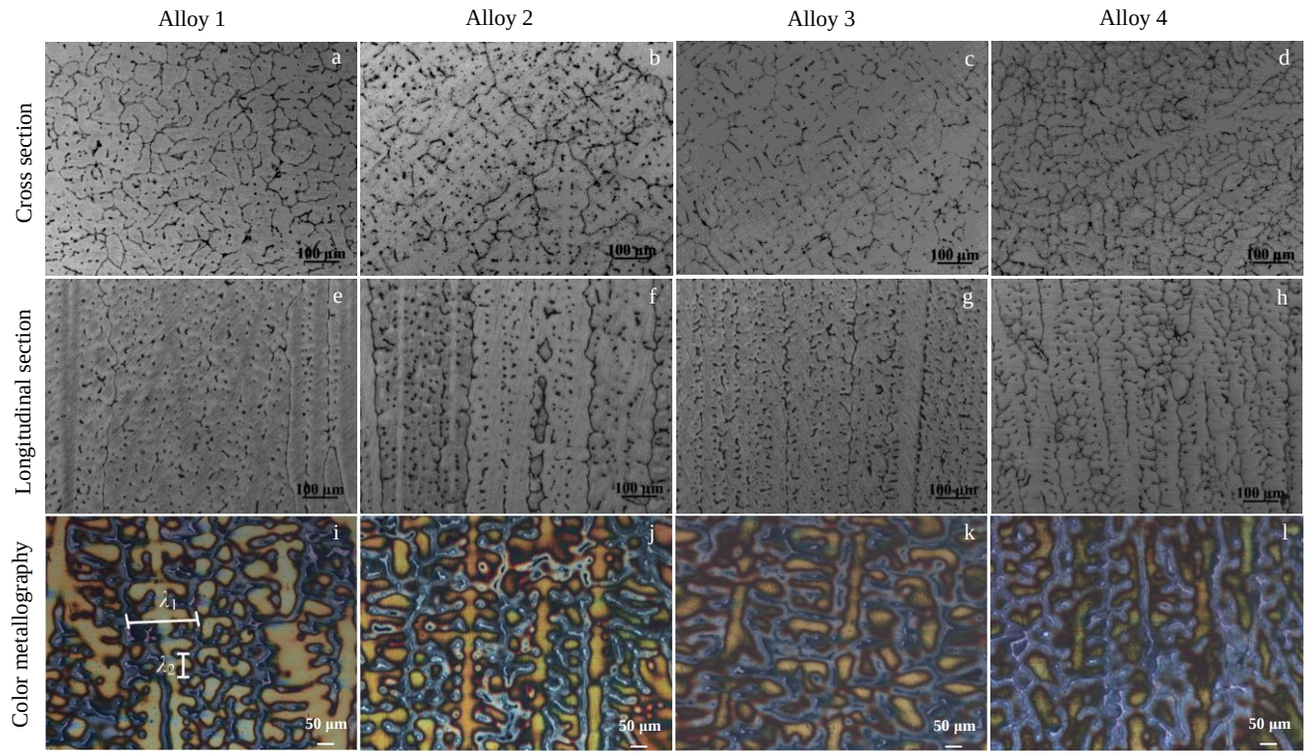

Fig.1 Cross section (a~d) and longitudinal section (e~h) microstructures and color metallographys (i~l) of alloy 1 (a, e, i), alloy 2 (b, f, j), alloy 3 (c, g, k) and alloy4 (d, h, l)

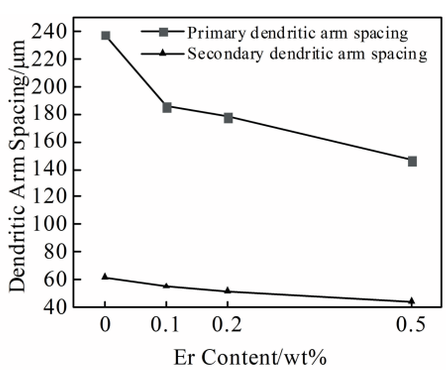

Fig.2 Primary and secondary dendrite arm spacing

and morphology of the second phase precipitated in the alloy differ greatly. Statistical analysis of the second phase content is displayed in Fig. 4. Compared with alloy 1, the content of second phase precipitated in alloy 2 and alloy 3 is significantly reduced, while the content of second phase precipitated in alloy 4 is increased to a certain extent.

After adding Er, the morphology of second phase changes obviously. Among them, the boundary of second phase in alloy 2 and alloy 3 is gradually rounded, and the content of second phase in the circular shape is greatly increased compared to alloy 1; the boundary of second phase in alloy 4 is sharper, and there are mainly irregular stripe-shaped second phases. The ratios of round-shape second phase in the alloys are shown in Fig.4. The ratio of the round-shape second phase in alloy 3 is the highest, 68.79%, which is 59.79% higher than 43.05% of alloy 1; alloy 4 has the lowest round-shape second phase ratio of 21.67%, which is 49.66% lower than that of alloy 1.

2.3 Hardness measurement

The hardness of alloys with different Er contents was measured, and the hardness values of the cross section and the longitudinal section of the alloy were also measured. The measurement results are shown in Fig. 5. As the Er content increases, the hardness value of the alloy gradually increases; the hardness value of the cross section increases from 1180 MPa to 1420 MPa, and that of the longitudinal section increases from 1380 MPa to 1540 MPa. The primary dendrite arm spacing and secondary dendrite arm spacing of the alloy decrease with the increase of the addition amount of Er element[31]. The grains become finer and the structure becomes denser, so the microhardness value of the alloy is improved. It can be seen that the hardness of the longitudinal section is higher than that of the cross section. This is because the longitudinal section of the alloy is oriented during directional solidification, and the longitudinal section structure is denser, so the hardness value of the longitudinal section is higher.

3 Discussion

3.1 Formation of Al_8Cu_4Er phase

Al_8Cu_4Er phase is precipitated in the alloy with adding Er element. The formation law of the alloy phase depends on the

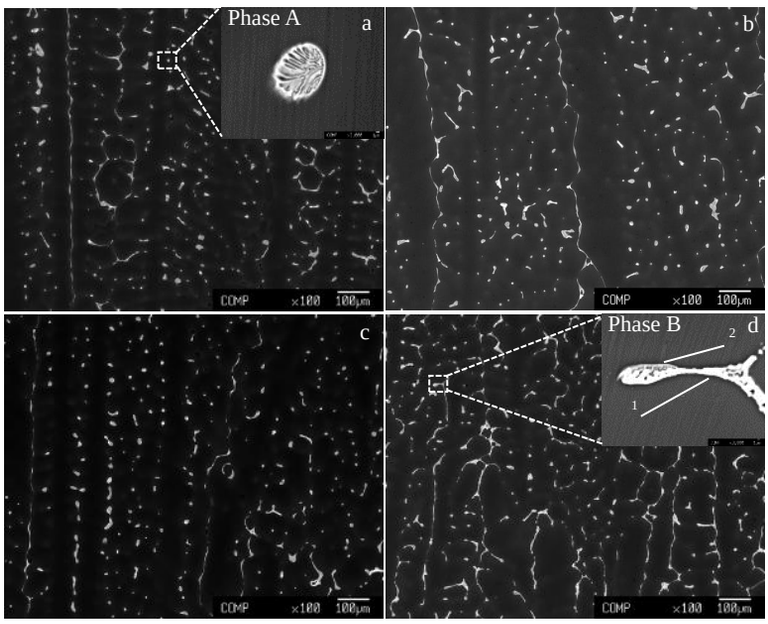

Fig.3 BSE images of longitudinal section of alloys: (a) alloy 1, (b) alloy 2, (c) alloy 3, and (d) alloy 4

Table 1 EDS analysis results of the second phase precipitates (at%)

Item	Al	Zn	Mg	Cu	Zr	Er	Phase
Phase A	45.05	18.38	23.08	12.29	0.01	-	AlZnMgCu
Phase B_1	71.71	6.21	0.26	17.86	0.00	3.96	Al_8Cu_4Er
Phase B_2	56.36	15.73	17.83	9.85	0.02	0.21	AlZnMgCu

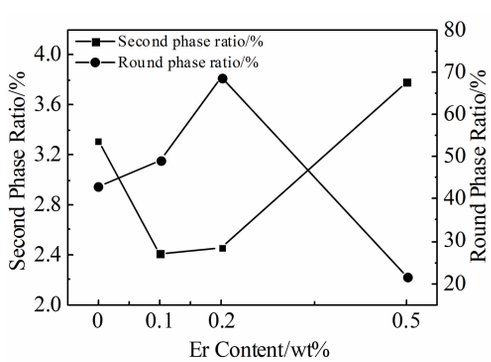

Fig.4 Statistical analysis results of second phase content in alloys

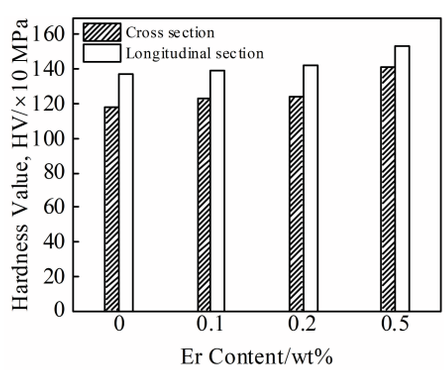

Fig.5 Hardness measurement results

interaction between the atoms in the alloy, and all the interactions between the atoms can be attributed to the interaction between the electrons. Among them, the theory of the interaction strength between the alloy elements can be used to judge the formation of the alloy phase law[32].

The theoretical formula of the interaction strength between two alloying elements is:

$$W = [0.15(r_A - r_B)/r_B]^2 + [(N_A - N_B)/0.4]^2 \quad (1)$$

where r_A and r_B are the atomic radius of solvent A and solute B, respectively; N_A and N_B are the electronegativity of solvent A and solute B, respectively.

According to the theory of interaction strength between alloy elements, the interaction strength of Er with Cu, Al, Zn, Mg, and Zr is 8.23, 5.39, 4.73, 2.30, and 1.63, respectively, which gradually decreases. The interaction strength of Er-Cu is the highest, indicating that the addition of Er will inhibit the solid solution of Cu, reduce the solid solubility of Cu in the α-Al matrix, and increase the tendency of forming compounds. Therefore, many Er- and Cu-rich second phases are found in the second phase of the alloy with Er addition. It is observed that the interaction strength of Er-Mg and Er-Zr is small, indicating that it is not easy to form a compound between Er and these two elements, which will promote the solid solution of these two elements.

In addition, the interaction strength of Er-Zn is 4.73, indicating that Er-Zn compound may form. However, due to the small amount of Er addition, this process is inhibited. Al_8Cu_4Er contains a small amount of Zn. Therefore, EDS

results of phase B_1 in Section 2.1 are explained.

3.2 Effects of Er on different second phases

The two main second phases generated in all alloys are Al_8Cu_4Er phase and T phase, with melting points of about 575 and 473 ℃, respectively. During the solidification process, as the temperature decreases, the Al_8Cu_4Er phase and the T phase are sequentially formed. In alloy 1, the main second phase is the T phase. In alloy 2, alloy 3, and alloy 4, due to the addition of the Er, the Al_8Cu_4Er phase is preferentially formed in the alloys, and more Cu participates in the reaction process with Er element, so the Cu contents of T phase in these alloys are reduced. According to the analysis result of Fig.4, the second phase morphology in alloy 1 is mainly round or irregular strips, and the content of round-shape second phase is 43.05%. After the addition of Er element, the ratio of round-shape second phase in the alloy changes significantly, and the ratio of round-shape second phase in alloy 3 is the largest, reaching 68.79%. The BSE images of the irregular strip-like second phase in alloy 1 and the round-shape second phase in alloy 3 are shown in Fig. 6a and 6b, respectively and the Cu content at each position is shown in Fig.6c. It is found that the Cu content at different positions of the T phase in alloy 1 changes greatly, and the Cu content in the round shape of alloy 3 does not change much, indicating that there is segregation of Cu element in the bright white of the irregular second phase in alloy 1. At the second phase boundary, a sharper phase boundary is formed. When the homogenization process cannot completely eliminate the second phase, the remaining sharp phase boundary often causes inconvenience in the subsequent processing of the alloy and affects the final performance of the product. By adding an appropriate amount of Er, the Al_8Cu_4Er phase formed in the alloy will reduce the Cu element content in the T phase, which plays a role of rounding the T phase boundary, then forming a large number of round T phases.

The morphology of the second phase of alloys with different compositions changes significantly with the addition of Er, and the morphology of the generated round T phases is

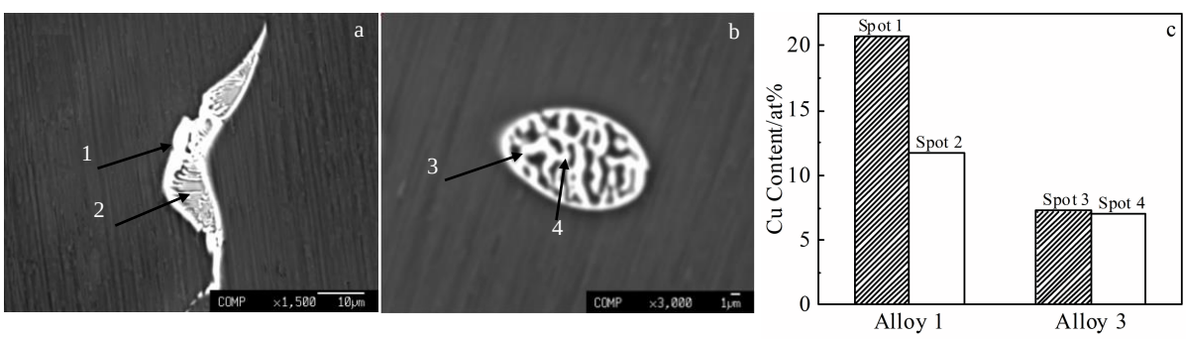

Fig.6 BSE images of irregular T phase in alloy 1 (a) and round T phase in alloy 3 (b); Cu content at various spots (c)

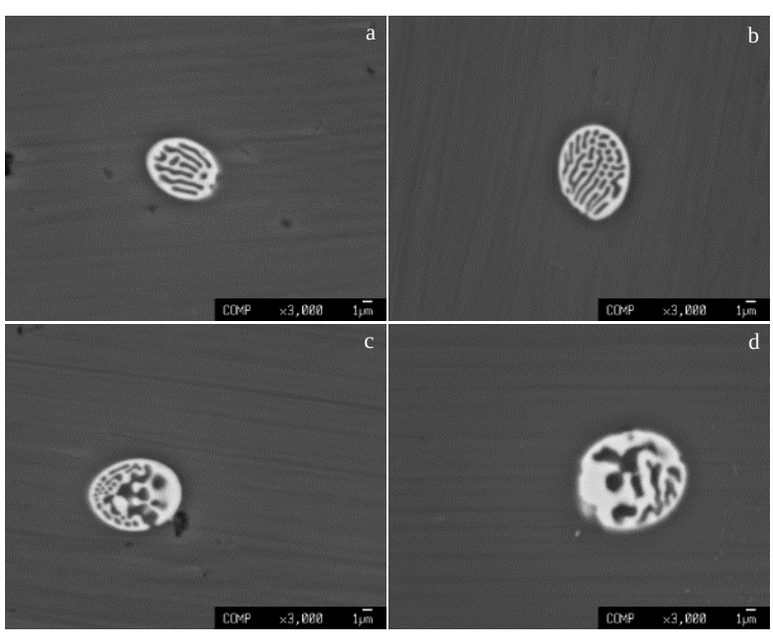

Fig.7 T phase morphologies of alloys with different compositions: (a) alloy 1, (b) alloy 2, (c) alloy 3, and (d) alloy 4

also different. The round T phases of the four alloys with different compositions are shown in Fig. 7. The difference in the content of Er element causes a significant change in the internal structure of the round T phase. The content of Cu element in the second phase with four different morphologies is shown in Fig. 8. According to the Jackson-Hunt model, when the degree of subcooling increases, the interlamellar spacing will become smaller, and the structure will become finer. After the addition of Er element, the alloy will precipitate Al_8Cu_4Er second phase, resulting in a change in the element content of the T phase of alloys with different compositions. Among them, the Cu element content has the largest degree of change, which greatly decreases, so the degree of component supercooling at the front edge of the solid-liquid interface is reduced, and the layer spacing should be increased. However, a small amount of Er element dissolved in the T phase act as an impurity element, and transform the eutectic planar growth to cell growth. The solid phase excludes impurities into the liquid at the front of the interface, and a small range of components will form supercooling. After adding 0.1wt% Er element, the increase degree of the component supercooling caused by the solid solution of Er element is greater than the decrease degree of the component supercooling caused by the reduction of the Cu element content, so the interlamellar spacing of the round second phase in alloy 2 becomes smaller and the structure is denser.

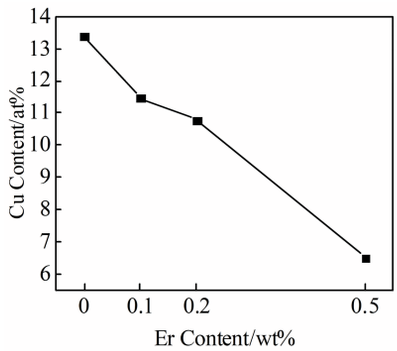

Fig.8 Cu element content of the round AlZnMgCu phase in Fig.7

As the Er element is continuously added, the decrease in the degree of supercooling caused by the continuous decrease in the Cu content dominates, so the interlamellar spacing of the round second phase in alloy 3 and alloy 4 increases.

The Al_8Cu_4Er phase (bright white part in the second phase) precipitated in alloys with different Er element contents is shown in Fig. 9. The Al_8Cu_4Er phase is located at the edge of the second phase or the connection point in the middle. Because the melting point of the Al_8Cu_4Er phase is higher than that of the T phase, it will precipitate before the T phase during the solidification process. Therefore, when the T phase

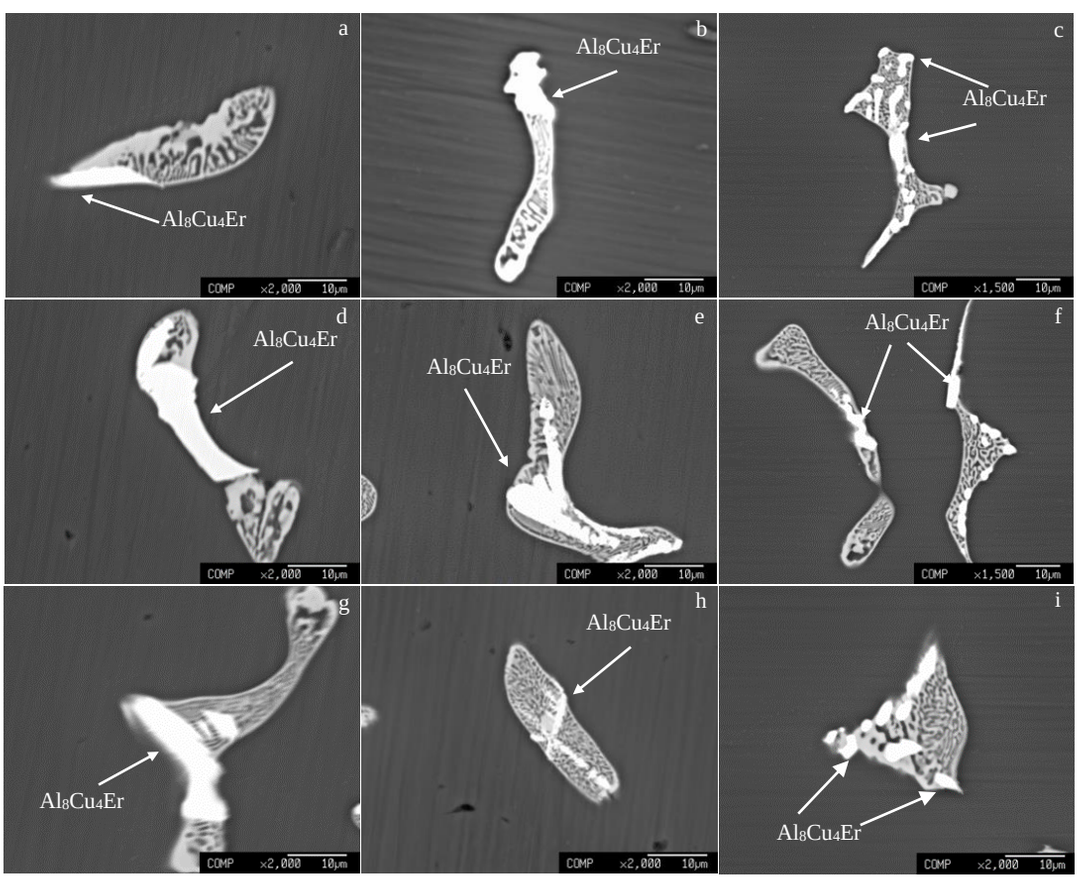

Fig.9 Al_8Cu_4Er phase morphologies in alloys with different Er contents: (a, d, g) alloy 2, (b, e, h) alloy 3, and (c, f, i) alloy 4

eutectic reaction occurs, the Al_8Cu_4Er phase provides nucleation sites with lower free energy, and these sites provide more favorable conditions for the eutectic phase to occur. Therefore, the T-phase eutectic reaction proceeds around the phase, and the macroscopically bright white Al_8Cu_4Er phase is in the edge of the T phase or the position where multiple T phases are connected. The small bright white Al_8Cu_4Er phase is completely encapsulated in the eutectic T phase due to its small size when providing the nucleation position.

3.3 Formation mechanism of circular second phase

The formation of the T phase (AlZnMgCu) is as follows, according to the non-equilibrium eutectic reaction formula:

$$L \rightarrow \alpha\text{-Al}+T(AlZnMgCu) \quad (2)$$

The two products produced by the reaction are the α-Al phase and the AlZnMgCu phase. As the reaction progresses, the two phases nucleate and grow alternately. During the participating of four elements in the reaction, the diffusion rate of Cu is the slowest and has the greatest influence on the whole reaction. When the α-Al phase nucleates, excess Cu is discharged from the crystal since the Cu content in the α-Al phase is less than that in the liquid phase, and the Cu content near the reaction interface increases, which promotes the AlZnMgCu phase to grow. The α-Al and AlZnMgCu phases alternately nucleate and grow, showing a network layered structure macroscopically. Because the diffusion rate of Cu element is slow, it is easy to segregate at the T phase boundary and easier to form a sharp phase boundary. When Er element is added, Cu element participates in the reaction of Er element. Therefore, in the reaction of forming T phase, the content of Cu element decreases accordingly. After the α-Al phase is formed, the Cu element discharged from the crystal to the liquid phase in reaction interface decreases. The ability to promote the formation of AlZnMgCu phase is reduced, and the Cu element is not easy to segregate. In order to reduce the free energy of the system, the macroscopic appearance is a round second phase, and there is a certain network layer structure inside.

After adding 0.5wt% Er element, the content of the second phase in the round shape is the smallest among the four alloys. This is because as the Er content increases, the number of Al_8Cu_4Er phases generated increases accordingly, which act as nuclei. The site makes the AlZnMgCu phase nucleate and grow around the Al_8Cu_4Er phase, and the macroscopic appearance is an irregular second phase shape.

4 Conclusions

1) In Al-Zn-Mg-Cu-Zr-xEr (x=0, 0.1, 0.2, 0.5, wt%) alloys, with the increase of Er content, the dendrite spacing becomes smaller while the number of dendrites increases. After adding 0.5wt% Er element, continuous dendrites are formed in the alloy.

2) Adding an appropriate amount of Er element can effectively reduce the precipitation degree of the second phase in the alloy, and can change the morphology of the second phase, so that the content of the second phase with round shape increases. However, when the addition amount is too large, the degree of precipitation of the second phase in the alloy is greatly increased, and the content of the round second phase is greatly reduced. The addition of Er element can improve the hardness of the alloy.

3) The Al_8Cu_4Er phase is formed in the alloy added with Er element, which reduces the Cu content in the T phase (AlZnMgCu), and changes the morphology of the T phase; and the internal structure changes accordingly.

References

1 Cong Fuguan, Zhao Gang, Tian Ni *et al*. *Light Alloy Fabrication Technology*[J], 2012, 10(3): 23

2 Zhou Wansheng, Yao Junshan. *Welding of Aluminum and Aluminum Alloys*[M]. Beijing: Machinery Industry Press, 2006: 3

3 Liu Jingan, Xie Shuisheng. *Application and Technical Development of Aluminum Alloy Materials*[M]. Beijing: Metallurgical Industry Press, 2011: 5

4 Heinz A, Haszler A, Keidel C. *Materials Science and Engineering A*[J], 2000, 280(1): 102

5 Mukhopadhyay A. *Transactions of the Indian Institute of Metals* [J], 2009, 62(2): 113

6 Jian Haigen, Jiangfeng, Xu Zhongyan *et al*. *Hot Working Technology*[J], 2006, 35(12): 61

7 Liu Bing, Peng Chaoqun, Wang Richu *et al*. *The Chinese Journal of Nonferrous Metals*[J], 2010, 20(9): 1705

8 Shen Chen, Sun Hui, Zhi Dongdong. *Nonferrous Metal Materials and Engineering*[J], 2018, 9(4): 70

9 Wang Shaohua, Meng Linggang, Yang Shoujie *et al*. *Transactions of Nonferrous Metals Society of China*[J], 2011, 21(7): 1449

10 Wu Hao, Wen Shengping, Huang Hui *et al*. *Materials Science and Engineering A*[J], 2017, 689: 313

11 Wu Hao, Wen Shengping, Lu Juntai *et al*. *Transactions of Nonferrous Metals Society of China*[J], 2017, 27(7): 1476

12 Wang Xudong, Nie Zuoren, Lin Shuangping *et al*. *Special Casting and Nonferrous Alloys*[J], 2009, 29(1): 76

13 Wang Ziyue, Chen Ziyong, Nie Zuoren *et al*. *Hot Working Technology*[J], 2015, 44(2): 118

14 Mehdi Malekan, Massoud Emamy, Nima Mossayebi. *Journal of Materials Engineering and Performance*[J], 2019, 29(5): 3432

15 Liu Shengdan, Li Chengbo, Ouyang Hui *et al*. *The Chinese Journal of Nonferrous Metals*[J], 2013, 23(4): 927 (in Chinese)

16 Zhang Xinming, Liu Wenjun, Liu Shengdan *et al*. *Materials Science and Engineering A*[J], 2011, 528(3): 795

17 Chen Songyi, Chen Kanghua, Peng Guosheng *et al*. *Materials and Design*[J], 2012, 35: 93

18 Li P Y, Xiong B Q, Zhang Y A *et al*. *The Chinese Journal of Nonferrous Metals*[J], 2011, 21(3): 513 (in Chinese)

19 Zhang Xinming, Liu Wenjun, Li Hongping *et al*. *The Chinese Journal of Nonferrous Metals*[J], 2011, 21(9): 2060 (in Chinese)

20 Li Peiyue, Xiong Baiqing, Zhang Yongan *et al*. *Transactions of*

Nonferrous Metals Society of China [J], 2012, 22(2): 268

21 Liu Ying, Zhu Baohong, Zhang Yongan *et al*. *Rare Metals*[J], 2012, 36(4): 529 (in Chinese)

22 Chandan Mondal, Mukhopadhyay A K, Raghu T *et al*. *Materials and Manufacturing Processes*[J], 2007, 22(4): 424

23 Liu Yan, Jiang Daming, Xie Wenlong *et al*. *Materials Characterization*[J], 2014, 93: 173

24 Clark D A, Johnson W S. *International Journal of Fatigue*[J], 2003, 25(2):159

25 Wang Haijun, Xu Ju, Kang Yonglin *et al*. *Journal of Alloys and Compounds*[J], 2014, 585(5): 19

26 Song R G, Dietzel W, Zhang B J *et al*. *Acta Materiala*[J], 2004, 52(16): 4727

27 Liu Guili, Fang Geliang. *Rare Metal Materials and Engineering* [J], 2009, 38(9):1598 (in Chinese)

28 Zhu Ranran, Zhang Yongan, Xiong Baiqing *et al*. *Journal of Aeronautical Materials*[J], 2012, 32(5): 37

29 Fang Hongjie, Sun Jie, Liu Hui *et al*. *Heat Treatment of Metals* [J], 2017, 42(4): 53

30 Chen Xiangkai, Li Xiangming. *Materials Reports*[J], 2019, 33 (5): 871

31 Emine Acer, Emin Çadırlı, Harun Erol *et al*. *Metallurgical and Materials Transactions A*[J], 2016, 47(6): 3040

32 Wang Jingtao, Cui Jianzhong, Ma Longxiang. *Journal of Xi'an University of Architecture and Technology, Natural Science Edition*[J], 1993, 25(4): 445

Er元素对定向凝固Al-Zn-Mg-Cu-Zr合金微观组织和共晶相形貌的影响

袁　帅，贾丽娜，张　虎

(北京航空航天大学 材料科学与工程学院，北京 100191)

摘　要：采用定向凝固方法制备了Al-Zn-Mg-Cu-Zr-*x*Er（*x*=0，0.1，0.2，0.5，质量分数，%）4种合金棒。利用光学显微镜（OM）、电子探针（EPMA）、能谱分析（EDS）和其他方法研究了铸态合金的微观组织和第二相形貌。结果表明：Er元素能增加Al-Zn-Mg-Cu-Zr合金定向凝固组织的枝晶数量，并能减小合金的一次枝晶臂间距和二次枝晶臂间距。适量Er元素能减少合金第二相的含量并有利于形成圆形第二相。生成的Al_8Cu_4Er相会降低T相（AlZnMgCu）中的Cu含量，起到圆润T相边界的作用，改变了T相的形貌和内部结构，并且Al_8Cu_4Er相能充当T相的形核位置，使得一部分T相围绕该相生长。Er的添加会提高合金的显微硬度。

关键词：Al-Zn-Mg-Cu；Er；微观组织；共晶相；第二相形貌

作者简介：袁　帅，男，1995年生，硕士，北京航空航天大学材料科学与工程学院，北京 100191，电话：010-82339256，E-mail：yuanshuai950123@163.com